Expression, purification and crystallization of an SLC16 monocarboxylate transporter family homologue specific for L-lactate

Sara Bonetti, Stephan Hirschi & Patrick D Bosshart[1]

[1] Institute of Biochemistry and Molecular Medicine, University of Bern, CH-3012 Bern, Switzerland

Corresponding author:
Patrick D Bosshart, Ph.D.
Institute of Biochemistry and Molecular Medicine
University of Bern
Bühlstrasse 28
CH-3012 Bern, Switzerland
Tel.: +41-31 631 41 12
Email: patrick.bosshart@ibmm.unibe.ch

Abstract

L-lactate plays an important role as metabolite and signaling molecule in eukaryotes and bacteria. Monocarboxylate transporters (MCTs) of the SLC16 solute carrier family are responsible for the transport of L-lactate across eukaryotic and bacterial cell membranes. Here we report an efficient protocol for the expression and purification of an SLC16 family homologue in milligram amounts. The purified protein is stable and can thus be used for biochemical and structural studies as shown by successful crystallization.

Keywords:

Expression of membrane proteins

L-lactate transporter

Membrane protein

Monocarboxylate transporter

Purification of membrane proteins

SLC16 family

Structure

Introduction

Monocarboxylate transporters (MCTs) of the SLC16 solute carrier family (TCID 2.A.1.13), which comprises 14 members in the human genome, mediate stereoselective transport of L-lactate across plasma membranes [1]. MCTs 1-4 have been experimentally verified as proton-coupled L-lactate transporters [1]. MCT1 (*SLC16A1*) is ubiquitously expressed, but its expression level is increased in L-lactate oxidizing cells (e.g., erythrocytes). MCT2 (*SLC16A7*) is found in the brain, kidney, liver, and in the testis, while the expression of MCT3 (*SLC16A8*) is restricted to the basal membrane of the retinal pigment and choroid plexus epithelia. MCT4 (*SLC16A3*) is localized in glycolytically active and anaerobic tissues and its expression is under the control of the hypoxia-inducible factor 1α [2]. While MCTs 1 and 2 are involved in L-lactate uptake (MCT1: K_M 3-5 mM, MCT2: K_M ~0.7 mM), MCT4 (K_M 20-35 mM) catalyzes the extrusion of accumulated L-lactate out of cells [1]. It has been shown that L-lactate plays an important role in cancer metabolism [3]. Due to metabolic disorder, certain cancer cells cannot cover their demand of energy by oxidative phosphorylation even under aerobic conditions. Therefore, they exhibit highly increased glycolysis rates resulting in the accumulation of L-lactate, which has to be shuttled out of the cell by overexpressed MCT4. In cancer tissue, the acidification of the tumor microenvironment resulting from co-transported protons is beneficial for tumor propagation and survival [4]. Furthermore, exported L-lactate serves as fuel for proliferating cancer cells that import L-lactate through overexpressed MCT1 [5]. Inhibiting the transport function of MCT1 and MCT4, which have complementary roles, has been proposed as a promising strategy for treating certain cancer types. This is reflected by clinical trials involving an MCT1 inhibitor (see AZD3965 at http://www.clinicaltrials.gov/) and a recent study that identified the antihypertensive drug syrosingopine as MCT4 inhibitor [6]. However, the

design of potent and highly selective inhibitors as well as the possibility of reliable molecular docking has been hampered by the lack of experimental structures of the SLC16 family in the past.

Using X-ray crystallography we have recently solved structures of a proton-coupled L-lactate transporting SLC16 homologue from *Syntrophobacter fumaroxidans* (SfMCT) with bound substrate (i.e., L-lactate) and inhibitor (i.e., thiosalicylate) [7]. The structures, which represent the first structural information of the SLC16 family, show SfMCT in the pharmacologically relevant outward-open conformation where the binding site is accessible from the extracellular side. Here we report a detailed overexpression and purification procedure to obtain milligram amounts of highly pure, stable and detergent-solubilized SfMCT. The purified protein can be used for structure determination as well as for biochemical and biophysical characterization.

Materials and Methods

Cloning

A major facilitator superfamily-type transporter from *Syntrophobacter fumaroxidans* (SfMCT, UniProt ID code **A0LNN5**) was identified as a bacterial homologue of human proton-dependent L-lactate transporting SLC16 members (i.e., MCT1, MCT2, MCT3, and MCT4) by searching the bacterial target database of the UniProt Knowledgebase on ExPASy using the BLAST algorithm (https://web.expasy.org/blast/). A codon-optimized version of SfMCT was synthesized for expression in *Escherichia coli* (GenScript) containing 5'-HindIII and 3'-XhoI restriction sites, which were used to ligate the gene into the pZUDF21-rbs-3C10His plasmid [8] for protein overexpression. For ligation of the SfMCT gene into the pEXT20 plasmid [9], which was used for bacterial uptake assays, the 5'-HindIII was replaced by a 5'-EcoRI restriction site using

polymerase chain reaction whereas the 3'-XhoI restriction site was kept. The resulting constructs (pZUDF21-rbs-SfMCT-3C10His and pEXT20-SfMCT-3C10His) contained a C-terminal human rhinovirus 3C (HRV 3C) protease cleavage site and a decahistidine-tag (His-tag) for affinity purification.

Bacterial uptake assay

For the bacterial uptake assay, *E. coli* JA202 (MC4100 *glcA::cat lldP::kan*) [10], which lacks the endogenous L-lactate transporters LldP and GlcA, was transformed with the empty plasmid (pEXT20-3C10His) or the plasmid encoding SfMCT (pEXT20-SfMCT-3C10His). The transformed strains were inoculated in 25 ml Luria Bertani (LB) Broth (VWR Life Science) supplemented with 100 µg/ml ampicillin and 50 µg/ml kanamycin, and grown overnight at 37°C and 180 rpm in an incubator shaker (Multitron, Infors HT). The overnight cultures were diluted 1:200 into LB Broth supplemented with 100 µg/ml ampicillin, and grown at 37ºC and 180 rpm in an incubator shaker. Protein expression was induced at OD_{600} ~0.5 by addition of isopropyl-β-D-thiogalactopyranoside (IPTG, Apollo Scientific) to a final concentration of 250 µM. After 4 h, bacteria were pelleted (5,200 x *g*, 10 min, room temperature) and resuspended in uptake buffer (20 mM Bis-Tris propane-HCl (pH 6.7), 250 mM KCl) to a bacteria density of OD_{600} 12. The assay volume of the uptake experiments was 50 µl, which included 20 µl of cell suspension (2.4×10^8 bacteria) and 30 µl of radiolabel master mix (22 µM sodium L-lactate spiked with [^{14}C(U)] L-lactic acid sodium salt ([^{14}C]L-lactate, American Radiolabeled Chemicals) to a specific activity of 0.15 Ci/mmol). The uptake experiments were performed in 2 ml reaction tubes (Eppendorf) at 30ºC under agitation (1,000 rpm, Thermomixer compact, Eppendorf). 900 µl of stop buffer (20 mM HEPES-NaOH (pH 7.5), 150 mM NaCl) were added at different time points (5-120 min) to terminate the uptake of L-lactate. Bacteria were immediately

pelleted by centrifugation (21,000 x *g*, 4 min, room temperature) and washed twice with 900 µl stop buffer by repeating the previous centrifugation step. 50 µl of a 5% (w/v) sodium dodecylsulfate (SDS) solution were added to lyse the bacteria overnight and to release the transported [^{14}C]L-lactate. Lysed bacteria were transferred into a white 96-well plate (OptiPlate, PerkinElmer) and 150 µl of scintillation cocktail (MicroScint 40, PerkinElmer) were added before measuring each reaction for 2 min with a scintillation counter (TopCount NXT, PerkinElmer).

Test expression of SfMCT in different E. coli strains and Western blot analysis

Different chemically competent *E. coli* strains (i.e., BL21(DE3), BL21(DE3) pLysS, BL21(DE3) Gold, BL21(DE3) RIPL, Rosetta(DE3), Rosetta2(DE3), Rosetta2(DE3) pLysS, C41(DE3), C43(DE3)) were transformed with pZUDF21-rbs-SfMCT-3C10His using heat shock (60 s at 42°C), followed by growth in 900 µl LB Broth for 1 h at 37°C under agitation (800 rpm, Thermomixer compact, Eppendorf). 25 ml of LB Broth supplemented with 100 µg/ml ampicillin and 36 µg/ml chloramphenicol (for strains BL21(DE3) pLysS, Rosetta(DE3), Rosetta2(DE3) and Rosetta2(DE3) pLysS) were inoculated with the transformed *E. coli* strains and grown overnight at 37°C in an incubator shaker (180 rpm, Multitron, Infors HT). The overnight cultures were diluted 1:200 in 50 ml LB Broth supplemented with 100 µg/ml ampicillin and grown at 37°C in an incubator shaker (180 rpm, Multitron, Infors HT) to an OD_{600} of ~0.9. At this point, IPTG was added to a final concentration of 250 µM to induce SfMCT expression. After four hours, 2 ml of expression culture were pelleted in 2 ml reaction tubes (21,000 x *g*, 10 min, room temperature), the supernatant was removed, and the pellet was stored at -20°C. For Western blot analysis the bacteria pellets were thawed and incubated with 600 µl of non-reducing sample buffer (60 mM Tris-HCl (pH 6.8), 10% (v/v) glycerol, 2% (w/v) SDS, 0.01% (w/v) bromophenol blue) for 30 min at 24°C under agitation

(800 rpm, Thermomixer compact, Eppendorf). The samples were then diluted twofold in non-reducing sample buffer and separated on a 14% SDS-PAGE gel. Subsequently, proteins were transferred to a methanol-activated polyvinylidene difluoride membrane (PVDF, Immobilon-P Transfer Membrane, Merck Millipore) using a semi-dry blotting system (Trans-blot SD Semi-Dry Transfer Cell, Bio-Rad) operated at 22 V for 25 min at room temperature. The transfer buffer (48 mM Tris, 39 mM glycine, 1.3 mM SDS, 20% (v/v) methanol) was freshly prepared. After the transfer, the PVDF membrane was rinsed with Tris-buffered saline (TBS; 10 mM Tris-HCl (pH 8), 150 mM NaCl) and incubated in 30 ml blocking solution (3% bovine serum albumin (BSA) in TBS) on an orbital shaker for 1 h at room temperature. After removing the blocking solution, the membrane was directly incubated with a mouse anti-His_5 primary antibody (Qiagen, catalogue number 34660) at a dilution of 1:3,000 in 30 ml blocking solution on an orbital shaker for 1 h at room temperature. After washing the PVDF membrane three times for 10 min with 30 ml TBS, it was incubated with a secondary goat anti-mouse IgG (H+L) HRP conjugate antibody (Bio-Rad, catalogue number 172-1011) at a dilution of 1:2,500 in 30 ml 5% (w/v) non-fat dry milk powder (Rapilait, Migros) in TBS on an orbital shaker for 1 h at room temperature. Finally, the PVDF membrane was washed four times for 10 min with 30 ml Tween-20-supplemented TBS (10 mM Tris-HCl (pH 8), 150 mM NaCl, 0.05% (v/v) Tween-20) followed by incubation in 6 ml electrochemiluminescence solution (Amersham ECL Western blotting Detection Reagents, GE Healthcare) for 2 min. Antibody-labelled proteins were detected by exposing X-ray films (Fujifilm) for 5 seconds.

Large-scale expression and membrane isolation

Based on test expressions using various *E. coli* strains (see **Test expression** section), *E. coli* BL21(DE3) pLysS was selected as expression host for large-scale expression of

SfMCT in an incubator shaker (Multitron, Infors HT). LB Broth supplemented with 100 µg/ml ampicillin and 36 µg/ml chloramphenicol was inoculated with transformed *E. coli* BL21(DE3) pLysS from a glycerol stock prepared from the test expression cultures and grown overnight at 37°C in an incubator shaker (180 rpm, Multitron, Infors HT). A typical SfMCT overexpression batch contained 30 l of LB Broth split into fifteen 5 l plain bottom Erlenmeyer flasks. The overnight culture was diluted 1:200 in 2 l LB Broth supplemented with 100 µg/ml ampicillin and grown at 37°C in an incubator shaker (180 rpm, Multitron, Infors HT) to an OD_{600} of ~0.9. At this point, 250 µM IPTG were added to induce SfMCT expression. After four hours, bacteria were harvested by centrifugation (10,000 x *g*, 6 min, 4°C). The resulting pellet was resuspended in ice-cold lysis buffer (45 mM Tris-HCl (pH 8), 450 mM NaCl) and pelleted again (10,000 x *g*, 25 min, 4°C). The final bacteria pellet was resuspended in lysis buffer and stored at -20°C until further use. For isolating the membranes, bacteria were thawed at room temperature and disrupted using a pre-cooled M-110P Microfluidizer (Microfluidics) operated at 1,500 bar during six passages. Unlysed bacteria were removed by low-speed centrifugation (10,000 x *g*, 10 min, 4°C) and the supernatant was then subjected to ultracentrifugation (200,000 x *g*, 90 min, 4°C). The resulting pellet was resuspended in lysis buffer, homogenized using a glass teflon homogenizer (Sartorius) and again subjected to ultracentrifugation (200,000 x *g*, 90 min, 4°C). Membranes were finally resuspended and homogenized in solubilization buffer (20 mM Tris-HCl (pH 8), 150 mM NaCl, 10% (v/v) glycerol) using a glass teflon homogenizer. Isolated and washed membranes were finally diluted to 100 mg/ml and stored at -80°C. Typically 0.25-0.5 g of membranes (i.e., wet weight) were obtained from 1 l of expression culture.

206 ***Purification of SfMCT***

207 Purification of SfMCT was performed at 4°C unless otherwise stated. Isolated and
208 washed membranes were thawed at room temperature and solubilized in solubilization
209 buffer (25 ml for membranes from 2 l of expression culture) containing 2% (w/v) *n*-
210 dodecyl-β-D-maltopyranoside (DDM, Glycon Biochemicals) by gentle agitation on a
211 magnetic stirrer for 2 h. Unsolubilized and aggregated material was removed by
212 ultracentrifugation (200,000 x *g*, 30 min, 4°C). The supernatant was diluted twofold
213 with detergent-free washing buffer (20 mM Tris-HCl (pH 8), 150 mM NaCl, 5 mM L-
214 histidine, 5% (v/v) glycerol) and incubated with nickel-nitrilotriacetate resin (Ni-NTA;
215 ProteinIso; 1 ml resin bed volume for solubilized membranes from 1 l of expression
216 culture) for 2 h under gentle stirring. The Ni-NTA resin was then transferred into a
217 glass chromatography column (Econo-Column, Bio-Rad) using a peristaltic pump
218 (Peristaltic Pump P-1, Pharmacia Fine Chemicals) operated at a flow rate of 4 ml/min.
219 The resin was washed with 25 column volumes of washing buffer (20 mM Tris-HCl
220 (pH 8), 150 mM NaCl, 5 mM L-histidine, 5% (v/v) glycerol, 0.03% (w/v) DDM) and
221 with 25 column volumes of size-exclusion chromatography (SEC) buffer (20 mM Tris-
222 HCl (pH 8), 150 mM NaCl, 0.03% (w/v) DDM) at a flow rate of 0.8 ml/min. 400 µl of
223 SEC buffer and 500 µg of His-tagged HRV 3C protease (BioVision, Milpitas, CA,
224 USA; stored in 20 mM Tris-HCl (pH 8.0), 300 mM NaCl, 50% (v/v) glycerol, 5 mM
225 β-mercaptoethanol) per 1 ml of column bed volume were added to the Ni-NTA in order
226 to elute SfMCT during overnight on-column cleavage on a rotational shaker. SfMCT
227 and unbound His-tagged HRV 3C protease were spin-eluted from the column (3,000 x
228 *g*, 3 min, 4°C) followed by reverse Ni-NTA purification to remove uncleaved SfMCT
229 and co-eluted His-tagged HRV 3C protease. For that purpose, the elution volume was
230 incubated with 150 µl bed volume Ni-NTA per mg of His-tagged HRV 3C protease for

10 min on a rotational shaker. The Ni-NTA resin was removed by passing the mixture over a disposable column (Wizard Midicolumns, Promega). Finally, aggregated proteins were removed by ultracentrifugation (150'000 x *g*, 20 min, 4°C).

Size-exclusion chromatography

Size-exclusion chromatography (SEC) was performed using a Superdex 200 10/300 GL column (GE Healthcare) that was connected to a fast protein liquid chromatography (FPLC) system (Äkta Purifier, GE Healthcare) operated at a flow rate of 0.5 ml/min. The column was equilibrated with 1.5 column volumes of SEC buffer (20 mM Tris-HCl (pH 8), 150 mM NaCl, 0.03% (w/v) DDM) before injecting 50 µg (100 µl, 0.5 mg/ml) of purified, DDM-solubilized SfMCT. The SfMCT elution profile was detected at an absorption wavelength of 280 nm and processed using the UNICORN software (GE Healthcare).

Gel electrophoresis

Denaturing SDS-PAGE was performed using a 14% SDS-PAGE gel where 20 µg of purified, DDM-solubilized SfMCT were loaded. The gel was stained with Coomassie Brilliant blue R-250 (AppliChem) to visualize the protein bands. Precision Plus Protein unstained standard (Bio-Rad) was used as a molecular weight marker. For Blue Native (BN)-PAGE, 20 µl of a 0.25 mg/ml SfMCT sample (i.e., a total of 5 µg) were mixed with BN-PAGE loading buffer (final concentration 50 mM BisTris-HCl (pH 7.2), 50 mM NaCl, 10% (w/v) glycerol) supplemented with 0.1% (w/v) DDM and 0.08% (w/v) Coomassie Brilliant blue G-250 (AppliChem). The SfMCT sample was loaded on a 4-16% BisTris NativePAGE gel (ThermoFisher). The gel was run using anode buffer (50 mM BisTris (pH 6.8), 50 mM Tricine (pH 6.8)) and dark blue cathode buffer (50 mM BisTris (pH 6.8), 50 mM Tricine (pH 6.8), 0.02% (w/v) Coomassie Brilliant blue G-250) at 150 V for the first 30 min and light blue cathode buffer (50 mM BisTris (pH

6.8), 50 mM Tricine (pH 6.8), 0.002% (w/v) Coomassie Brilliant blue G-250) for the following 80 min at 250 V. The gel tank was suspended in ice water during the whole run. Thyroglobulin (669 kDa), ferritin (440 kDa), lactate dehydrogenase (140 kDa), and bovine serum albumin (66 kDa) were used as molecular weight markers.

Determination of the thermostability of SfMCT

The thermostability of SfMCT was determined as previously described using a combination of heat denaturation and SEC analysis [11,12]. Purified, DDM-solubilized SfMCT was diluted to 0.5 mg/ml (~11 µM) using SEC buffer (20 mM Tris-HCl (pH 8), 150 mM NaCl, 0.03% (w/v) DDM). Aliquots of 150 µl were incubated in 200 µl reaction tubes (Sarstedt) for 2 min at 4°C and 10 min at different temperatures (4-60°C) in a thermocycler (SensoQuest GmbH). Heat-treated samples were centrifuged (18,000 x *g*, 1 min, room temperature) to remove aggregates. 100 µl (i.e., 50 µg, 1.1 nmol) of SfMCT were loaded on a Tricorn 5/150 column (GE Healthcare) packed with Superdex 200 PG resin (GE Healthcare), which was connected to an FPLC system (Äkta Purifier, GE Healthcare) and which was equilibrated with two column volumes of SEC buffer. SfMCT was eluted using SEC buffer at a flow rate of 0.55 ml/min and the elution profiles were detected at an absorption wavelength of 280 nm and processed using the UNICORN software (GE Healthcare). The maximum of the elution peak was plotted versus the incubation temperature to assemble a melting curve (i.e., absorption vs. temperature). Three independent melting curves, each consisting of triplicate data points, were normalized by fitting a sigmoidal model curve to each melting curve. Absorption values were normalized with respect to the determined upper plateau value, i.e., the fitted upper plateau value corresponds to 100%. The arithmetic average of three independent, normalized experiments was calculated. The melting temperature (T_m) of purified, DDM-solubilized SfMCT was determined by fitting a sigmoidal curve to the

281 averaged, normalized melting curve using Prism6 (GraphPad Software) and using the
282 temperature at which the normalized absorption dropped to 50% as T_m.

283 ***Crystallization***

284 SfMCT was purified as described in the **Purification of SfMCT** section with the
285 exception that DDM was replaced by *n*-nonyl-β-D-glucopyranoside (NG, Glycon
286 Biochemicals). For solubilization, 4% (w/v) and for all purification steps 0.4% (w/v)
287 NG were used. Purified, NG-solubilized SfMCT was concentrated to 8 mg/ml using a
288 50,000 Da molecular weight cut-off ultrafiltration device (Vivaspin 2, SARTORIUS
289 Stedim Biotech). The ultrafiltration device was centrifuged at 1,000 x *g* in 20 min
290 intervals followed by resuspending the concentrate to avoid detergent gradient
291 formation. Aggregated protein was removed by ultracentrifugation (150,000 x *g*, 30
292 min, 4 ºC). The final glycerol concentration (see **Purification of SfMCT** section) was
293 adjusted to 2.9% (v/v) and the sample was incubated on ice for 1 h prior to
294 crystallization. A Mosquito Crystal Robot (TTP Labtech) was used to mix concentrated
295 SfMCT with reservoir solution (50 mM HEPES-NaOH (pH 7), 5 mM $ZnBr_2$, 30% (v/v)
296 Jeffamine ED-2003). Crystallization trials were performed using the sitting-drop vapor-
297 diffusion method in 96-well 3-drop polystyrene crystallization plates (SWISSCI)
298 covered by transparent foils (AMPLIseal, Greiner Bio-One). After one day of
299 incubation at 18 ºC small crystals appeared, which reached maximal size after one
300 week. Crystals were flash frozen in liquid nitrogen.
301
302
303
304
305

Results and discussion

Functional characterization of SfMCT

SfMCT was identified as a bacterial homologue of the human proton-dependent L-lactate transporting SLC16 members (i.e., MCTs 1-4). It shares 25 and 27% amino acid sequence identity, and 51 and 57% sequence similarity with human MCT1 and MCT4 [7]. SfMCT was cloned into the pEXT20 expression plasmid and expressed in *E. coli* JA202 [10] to verify that it mediates the transport of L-lactate. A significantly higher uptake of [^{14}C]L-lactate into SfMCT-overexpressing bacteria was measured over time compared with the uptake into bacteria that were transformed with an empty control plasmid (Fig. 1). The net uptake signal of SfMCT, which was calculated by subtracting the uptake into control plasmid-carrying bacteria from the uptake into SfMCT-overexpressing bacteria, clearly shows that SfMCT transports L-lactate. Using the *E. coli* JA202 strain, which lacks the endogenous transporters LldP and GlcA, was essential because their L-lactate transport activity would obscure the uptake signal through SfMCT.

Figure 1

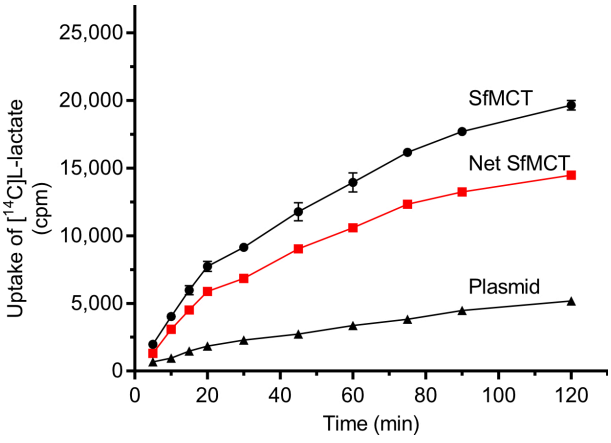

Figure 1: Time-dependent uptake of [^{14}C]L-lactate (13 µM) into SfMCT-expressing and plasmid transformed *E. coli* JA202 cells. The net uptake signal of SfMCT (red squares) was calculated by subtracting the uptake into control plasmid-carrying bacteria

(black triangles) from the uptake into SfMCT-overexpressing bacteria (black circles), Data are represented as mean ± SEM from a representative triplicate experiment.

Test-expression of SfMCT

Expression of SfMCT was tested in different *E. coli* strains to identify a suitable expression host for large-scale expression. In these strains, which contain the λ DE3 lysogen that carries the gene for the T7 RNA polymerase, heterologous expression of SfMCT can be induced by IPTG and they have been successfully used for the overproduction of membrane proteins in the past [13]. Almost no expression was detected in *E. coli* BL21(DE3) and *E. coli* Rosetta(DE3) (Fig. 2, lanes 1 and 5). Interestingly, the expression was significantly higher in *E. coli* BL21(DE3) pLysS (Fig. 2, lane 2), which carries the pLysS plasmid encoding the T7 lysozyme that prevents leaky expression in the absence of the inducer IPTG. A similar increase in expression in the presence of the pLysS plasmid was observed in *E. coli* Rosetta2(DE3) pLysS that showed the highest expression level among all tested strains as judged by Western blotting (Fig. 2, lanes 6 and 7). However, the high expression level in *E. coli* Rosetta2(DE3) pLysS was accompanied by high molecular weight aggregates that became visible as smears on the Western blot. Thus, this strain might not be optimal for obtaining stable and homogenous SfMCT as required for crystallization despite its high protein production capacity. A band at a molecular weight of ~70 kDa indicates SfMCT dimers whereas no low molecular weight bands were detected that would have indicated proteolytic degradation during protein expression. Finally, *E. coli* BL21(DE3) pLysS was selected as the preferred strain for overexpression of SfMCT because of the expected expression level and because this strain has been successfully used for the production of membrane proteins for structural analysis [13].

Figure 2

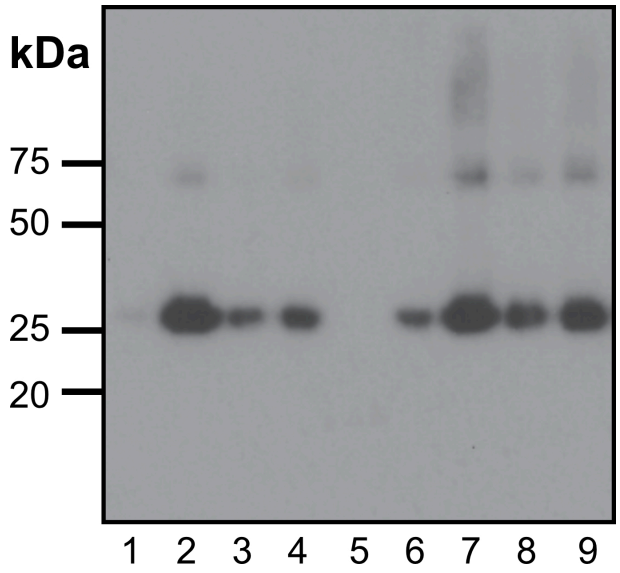

Figure 2: Western blot of SfMCT expressed in different *E. coli* strains. Equal volumes of overexpression cultures were loaded on a 14% SDS-PAGE gel and detected using a mouse anti-His_5 and a goat anti-mouse IgG (H+L) HRP conjugate antibodies. **1** BL21(DE3), **2** BL21(DE3) pLysS, **3** BL21(DE3) Gold, **4** BL21(DE3) RIPL, **5** Rosetta(DE3), **6** Rosetta2(DE3), **7** Rosetta2(DE3) pLysS, **8** C41(DE3), **9** C43(DE3).

Purification and characterization of SfMCT

We have established an efficient protocol for the purification of SfMCT that can be used for its biochemical characterization and crystallization. The cytosolic fraction was separated from SfMCT-containing membranes after bacteria lysis in order to reduce the amount of unspecific binding to the Ni-NTA resin. Isolated membranes were washed with a high-salt buffer (e.g., 45 mM Tris-HCl (pH 8), 450 mM NaCl) to reduce the amount of soluble and membrane-associated contaminants that might compete with His-tagged SfMCT for binding to the Ni-NTA resin [14]. According to our expression and membrane preparation protocol 0.25-0.5 g of washed bacterial membranes (i.e., wet weight) were obtained from 1 l of expression culture (Table 1). Efficient solubilization was achieved when membranes from 2 l expression culture were solubilized in a volume of 25 ml solubilization buffer using 2% (w/v) DDM. Elution of SfMCT by HRV 3C on-column proteolytic cleavage yielded pure protein as judged by

374 Coomassie-stained SDS-PAGE (Fig. 3a) where SfMCT migrated at a molecular weight
375 of ~30 kDa, which is lower than the amino acid sequence-based molecular weight of
376 ~45 kDa. Such discrepancies have been previously reported and are commonly
377 observed for membrane proteins [15-18]. A second and weaker band at ~70 kDa was
378 present, which was also observed on Western blots of bacteria expressing SfMCT (Fig.
379 2). Therefore, this band represents an SfMCT population and it does not originate from
380 a co-purified contaminant. The yield of the presented SfMCT purification procedure is
381 1.5-2 mg of SfMCT per liter of expression culture (Table 1).

382 The observed SfMCT population at ~70 kDa, which approximately corresponds
383 to twice the mass of the main population, might lead to the speculation that SfMCT
384 forms a dimer when expressed in *E. coli* and purified in DDM. This oligomeric state
385 might then be disrupted by the denaturing environment of SDS-PAGE. To address this
386 issue, DDM-purified SfMCT was analyzed by BN-PAGE where the oligomeric state
387 of membrane proteins is maintained during gel electrophoresis [16]. SfMCT migrated
388 as a single band at 85-95 kDa (Fig. 3b), which is the typical mass of a DDM-solubilized,
389 monomeric membrane transporter observed in BN-PAGE [15,17]. Furthermore, SEC
390 was performed to further assess the oligomeric state of DDM-solubilized SfMCT and
391 to verify the homogeneity of the sample. The chromatogram of SfMCT contains a
392 single peak at an elution volume of 12.7 ml indicating that the presented purification
393 procedure yielded a monodisperse membrane protein sample (Fig. 3c). The elution
394 volume is similar to the peak position of the monomeric, DDM-purified major
395 facilitator superfamily transporter LacY, which has a similar molecular weight
396 (SfMCT: ~45 kDa, LacY: ~48 kDa) [8]. Dimeric, DDM-purified membrane proteins of
397 similar monomer weight elute at significantly lower volumes [8]. In summary, we have
398 shown by BN-PAGE and SEC that SfMCT is a monomer when expressed in *E. coli* and

purified in DDM. The species that migrates at a molecular weight of ~70 kDa reflects most probably to unspecific and SDS-PAGE induced aggregation of SfMCT.

Thermostability of a purified, detergent-solubilized membrane protein can be a critical parameter for crystallization since it is generally exposed to temperatures higher than 4°C during crystal growth. The thermostability of SfMCT was determined using a previously described approach involving a combination of heat denaturation and SEC analysis [11,12]. An apparent melting temperature (T_m) of 46°C (95% confidence interval: 45.9 – 46.1°C) was measured for DDM-solubilized SfMCT (Fig. 3d), which is in the range of values that were previously published for other membrane proteins [11,19].

Figure 3

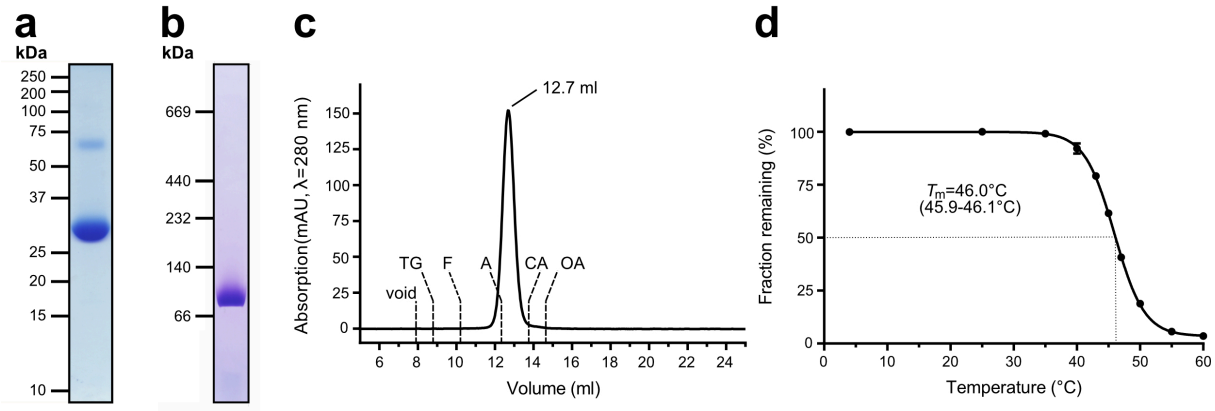

Figure 3: Biochemical and biophysical characterization of DDM-purified SfMCT. **(a)** Coomassie-stained 14% SDS-PAGE gel of purified SfMCT (20 µg of protein loaded). Denatured SfMCT runs as a prominent band at ~30 kDa and as a minor second band at ~70 kDa. **(b)** 4-16% BisTris NativePAGE linear gradient gel of purified SfMCT (5 µg of protein loaded). DDM-solubilized SfMCT migrates at 85-95 kDa. **(c)** SEC elution profile of purified SfMCT (50 µg) in SEC buffer. A monodisperse elution peak was detected at 12.7 ml. Void volume and retention volumes are indicated for the following standard proteins: thyroglobulin (TG, 669 kDa), ferritin (F, 440 kDa), aldolase (A, 158 kDa), conalbumin (CA, 75 kDa), and ovalbumin (OA, 43 kDa). **(d)** Melting curve of SfMCT. The solid line represents the fitted sigmoidal curve that was used to determine the melting temperature (T_m). 95% confidence interval values are indicated below the T_m values. Data are represented as mean ± SD from triplicates.

Table 1 SfMCT overexpression and purification table. Yield obtained from one liter of expression culture are indicated.

Purification step	Yield
Bacteria pellet	1.5-2 g
Membrane isolation	0.25-0.5 g
HRV 3C elution in DDM	1.5-2 mg
HRV 3C elution in NG	0.8-1 mg

Crystallization of SfMCT

Although pure, homogenous and thermostable SfMCT was obtained when purified in DDM, no crystals appeared in any crystallization screens. Therefore, SfMCT was also solubilized and purified in other uncharged maltoside-based (i.e., *n*-undecyl-β-D-maltopyranoside UDM, *n*-decyl-β-D-maltopyranoside DM, *n*-nonyl-β-D-maltopyranoside NM, *n*-octyl-β-D-maltopyranoside OM, 7-cyclohexyl-1-heptyl-β-D-maltopyranoside Cymal-7, 6-cyclohexyl-1-hexyl-β-D-maltopyranoside Cymal-6, 5-cyclohexyl-1-pentyl-β-D-maltopyranoside Cymal-5) and glucoside-based (*n*-nonyl-β-D-glucopyranoside NG, *n*-octyl-β-D-glucopyranoside OG) detergents at concentrations shown in Table 2 and crystallization trials were performed. Trapezoid-shaped crystals, which were suitable for collecting high-quality X-ray diffraction data [7], only grew when SfMCT was solubilized and purified in *n*-nonyl-β-D-glucopyranoside (NG) (Fig. 4a). Different commercial screens were used for initial crystallization trials. Small crystals (<20 μm) grew in only one condition of the commercial MemGold screen (80 mM HEPES-NaOH (pH 7), 2 mM $ZnSO_4$, 25% (v/v) Jeffamine ED-2001). This initial hit condition had to be optimized to obtain larger crystals (50 mM HEPES-NaOH (pH 7), 5 mM $ZnBr_2$, 30% (v/v) Jeffamine ED-2003). The presence of Zn^{2+} cations was essential for crystal growth. In contrast to DDM, NG

445 has a delipidating effect on ternary complexes (i.e., membrane protein, lipid, and
446 detergent) and forms significantly smaller micelles [8]. This might be beneficial for
447 promoting interactions between NG-solubilized SfMCT leading to well-ordered
448 crystals as observed for other NG-solubilized members of the major facilitator
449 superfamily [20,21]. Crystals grew on the bottom surface of the polystyrene
450 crystallization plates and had to be gently detached by touching the crystals at the long
451 side of the trapezoid with a cryo-loop.

452 The quality of the obtained crystals made it possible to determine the first
453 crystal structure of an SLC16 family member at 2.54 Å resolution [7]. SfMCT contains
454 12 TMs and adopts the typical major facilitator superfamily fold [22,23], where TMs
455 1-6 and TMs 7-12 form an N- and C-terminal six-helix bundle, which are related to
456 each other by a pseudo-twofold symmetry axis (Fig. 4b, grey dashed line). The structure
457 shows SfMCT in an outward-open conformation with a central, conical cavity that is
458 open to the periplasmic side (Fig. 4b, star). The obtained crystals belonged to the space
459 group $P2_12_12$ with unit cell parameters of a = 106.77 Å, b = 200.54 Å, c = 64.56 Å and
460 $\alpha = \beta = \gamma = 90°$. The asymmetric unit (Fig. 4c, dashed box) contained two SfMCT
461 molecules and had a Matthews coefficient of 3.92 $Å^3$/Da, which corresponds to a
462 solvent content of ~69% [24]. Such a high solvent content is often observed for
463 membrane protein crystals, and is attributed to the presence of ternary complexes
464 consisting of membrane proteins, detergents and lipids [25]. This can reduce protein-
465 protein interactions and results in fragile membrane protein crystals. The two SfMCT
466 molecules are tilted with respect to each other and make a crystal contact over TM12
467 (Fig. 4c, triangle). Extracellular loops connecting TM7 and TM8 of two SfMCT
468 monomers of adjacent asymmetric units form a second crystal contact (Fig. 4c, blue
469 arrow), while a third crystal contact exists between the loop enclosed by TM6 and TM7,

and the N-terminal end of TM10 (Fig. 4c, black arrow). The C-terminus of one SfMCT molecule is located in the periplasmic cavity of an SfMCT molecule located of a neighboring asymmetric unit thereby forming a fourth crystal contact (Fig. 4c, dashed circle). This contact highlights the importance of proteolytic His-tag removal since this affinity-tag would impede this crystal contact, which is highlighted by the fact that only HRV 3C cleaved protein resulted in crystal growth.

Conclusion

We have provided a protocol for the efficient overexpression and purification of the L-lactate transporting SLC16 homologue SfMCT. Following this protocol pure, homogenous and thermostable protein can be obtained at quantities that allow biochemical and biophysical characterization as well as crystallization and structure determination.

Figure 4

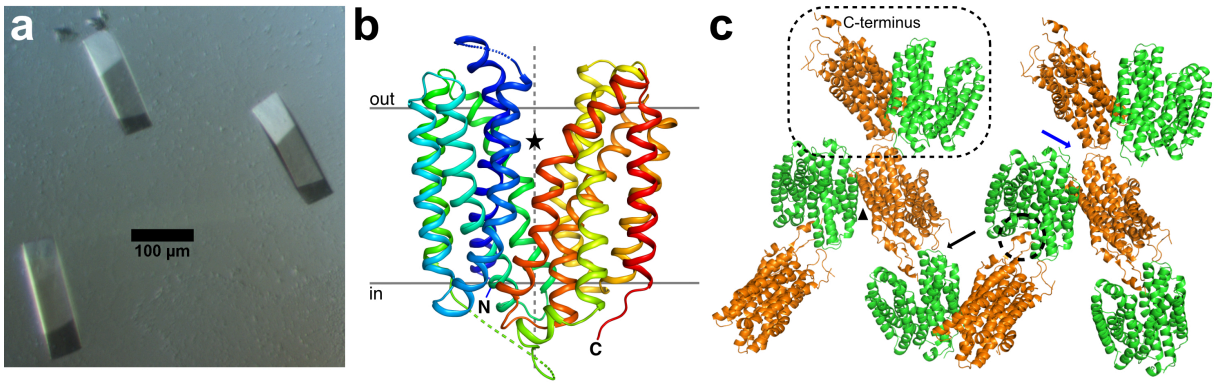

Figure 4: Crystallization of NG-solubilized SfMCT. (a) The micrograph shows typical trapezoid-shaped crystals of SfMCT. (b) Overall structure of SfMCT in the outward-open conformation. The central, conical cavity is highlighted by the asterisk and the grey, vertical broken line indicates the pseudo-twofold symmetry axis. N- and C-termini are labeled. Parts of the loops connecting TM1 and TM2, TM5 and TM6 as well as TM6 and TM7 could not be fully traced and are therefore represented by broken lines. The model of SfMCT is colored based on rainbow coloring scheme from blue (N-terminus) to red (C-terminus). (c) Crystal packing and contacts of SfMCT in space group $P2_12_12$. An asymmetric unit is highlighted by the dashed box. Crystal contacts are indicated by arrows, a triangle and a dashed circle.

Table 2 Detergent concentrations used for solubilization and purification of SfMCT. All values are taken from https://www.anatrace.com/. The critical micelle concentration is abbreviated by CMC.

Detergent	Molecular weight	CMC		Solubilization		Purification	
	g/mol	% (w/v)	mM	% (w/v)	mM	% (w/v)	mM
DDM	510.6	0.0087	0.17	2	39.17	0.03	0.59
UDM	496.9	0.029	0.59	2	40.25	0.1	2.01
DM	482.6	0.087	1.8	2	41.44	0.3	6.22
NM	468.5	0.28	6	4	85.38	0.4	13.05
OM	454.4	0.89	19.5	4	88.03	1.5	33.01
Cymal-7	522.5	0.0099	0.19	2	38.28	0.05	0.96
Cymal-6	508.5	0.028	0.56	2	39.33	0.1	1.97
Cymal-5	494.5	0.12-0.25	2.4-5.0	3	60.67	0.4	8.09
NG	306.4	0.2	6.5	4	130.55	0.4	13.05
OG	292.4	0.53-0.58	18-20	4	136.80	1	34.20

Conflicts of interest

The authors declare that they have no conflict of interest.

Acknowledgements

We thank the staff of the SLS (Paul Scherrer Institute) X06SA beamline for excellent support and advice. Financial support from the University of Bern, the Swiss National Science Foundation (grant 310030_184980) and the NCCR TransCure is kindly acknowledged.

References

[1] A.P. Halestrap, The SLC16 gene family - structure, role and regulation in health and disease, Mol. Aspects Med. 34 (2013) 337–349. doi:10.1016/j.mam.2012.05.003.

[2] M.S. Ullah, A.J. Davies, A.P. Halestrap, The plasma membrane lactate transporter MCT4, but not MCT1, is up-regulated by hypoxia through a HIF-1α-dependent mechanism, J. Biol. Chem. 281 (2006) 9030–9037. doi:10.1074/jbc.M511397200.

[3] I. San-Millán, G.A. Brooks, Reexamining cancer metabolism: lactate production for carcinogenesis could be the purpose and explanation of the Warburg Effect, Carcinogenesis. 60 (2016) 127–133. doi:10.1093/carcin/bgw127.

[4] S. Romero-Garcia, M.M.B. Moreno-Altamirano, H. Prado-Garcia, F.J. Sánchez-García, Lactate contribution to the tumor microenvironment: mechanisms, effects on immune cells and therapeutic relevance, Front. Immunol. 7 (2016) 52. doi:10.3389/fimmu.2016.00052.

[5] P. Sonveaux, F. Végran, T. Schroeder, M.C. Wergin, J. Verrax, Z.N. Rabbani, et al., Targeting lactate-fueled respiration selectively kills hypoxic tumor cells in mice, J. Clin. Invest. 118 (2008) 3930–3942. doi:10.1172/JCI36843.

[6] D. Benjamin, D. Robay, S.K. Hindupur, J. Pohlmann, M. Colombi, M.Y. El-Shemerly, et al., Dual inhibition of the lactate transporters MCT1 and MCT4 is synthetic lethal with metformin due to NAD^+ depletion in cancer cells, Cell Rep. 25 (2018) 3047–3058. doi:10.1016/j.celrep.2018.11.043.

[7] P.D. Bosshart, D. Kalbermatter, S. Bonetti, D. Fotiadis, Mechanistic basis of L-lactate transport in the SLC16 solute carrier family, Nat. Commun. 10 (2019) 76. doi:10.1038/s41467-019-10566-6.

[8] H. Ilgü, J.-M. Jeckelmann, M.S. Gachet, R. Boggavarapu, Z. Ucurum, J. Gertsch, et al., Variation of the detergent-binding capacity and phospholipid content of membrane proteins when purified in different detergents, Biophys. J. 106 (2014) 1660–1670. doi:10.1016/j.bpj.2014.02.024.

[9] D.M. Dykxhoorn, R. St Pierre, T. Linn, A set of compatible tac promoter expression vectors, Gene. 177 (1996) 133–136. doi:10.1016/0378-1119(96)00289-2.

[10] M.F. Núñez, M.T. Pellicer, J. Badía, J. Aguilar, L. Baldomà, The gene *yghK* linked to the *glc* operon of *Escherichia coli* encodes a permease for glycolate that is structurally and functionally similar to L-lactate permease, Microbiology. 147 (2001) 1069–1077. doi:10.1099/00221287-147-4-1069.

[11] R. Mancusso, N.K. Karpowich, B.K. Czyzewski, D.-N. Wang, Simple screening method for improving membrane protein thermostability, Methods. 55 (2011) 324–329. doi:10.1016/j.ymeth.2011.07.008.

[12] H. Ilgü, J.-M. Jeckelmann, C. Colas, Z. Ucurum, A. Schlessinger, D. Fotiadis, Effects of mutations and ligands on the thermostability of the L-arginine/agmatine antiporter AdiC and deduced insights into ligand-binding of human L-type amino acid transporters, Int. J. Mol. Sci. 19 (2018) 918. doi:10.3390/ijms19030918.

[13] G. Hattab, D.E. Warschawski, K. Moncoq, B. Miroux, *Escherichia coli* as host for membrane protein structure determination: a global analysis, Sci. Rep. 5 (2015) 618. doi:10.1038/srep12097.

[14] P.J. Werten, L. Hasler, J.B. Koenderink, C.H. Klaassen, W.J. de Grip, A. Engel, et al., Large-scale purification of functional recombinant human aquaporin-2, FEBS Lett. 504 (2001) 200–205. doi:10.1016/s0014-5793(01)02703-x.

[15] N. Reig, C. del Rio, F. Casagrande, M. Ratera, J.L. Gelpí, D. Torrents, et al., Functional and structural characterization of the first prokaryotic member of the L-amino acid transporter (LAT) family: a model for APC transporters, J. Biol. Chem. 282 (2007) 13270–13281. doi:10.1074/jbc.M610695200.

[16] F. Casagrande, M. Ratera, A.D. Schenk, M. Chami, E. Valencia, J.M. Lopez, et al., Projection structure of a member of the amino acid/polyamine/organocation transporter superfamily, J. Biol. Chem. 283 (2008) 33240–33248. doi:10.1074/jbc.M806917200.

[17] F. Casagrande, D. Harder, A. Schenk, M. Meury, Z. Ucurum, A. Engel, et al., Projection structure of DtpD (YbgH), a prokaryotic member of the peptide transporter family, J. Mol. Biol. 394 (2009) 708–717. doi:10.1016/j.jmb.2009.09.048.

[18] A. Rath, M. Glibowicka, V.G. Nadeau, G. Chen, C.M. Deber, Detergent binding explains anomalous SDS-PAGE migration of membrane proteins, Proc. Natl. Acad. Sci. U S A. 106 (2009) 1760–1765. doi:10.1073/pnas.0813167106.

[19] E. Nji, Y. Chatzikyriakidou, M. Landreh, D. Drew, An engineered thermal-shift screen reveals specific lipid preferences of eukaryotic and prokaryotic membrane proteins, Nat. Commun. 9 (2018) 172. doi:10.1038/s41467-018-06702-3.

[20] S. Dang, L. Sun, Y. Huang, F. Lu, Y. Liu, H. Gong, et al., Structure of a fucose transporter in an outward-open conformation, Nature. 467 (2010) 734–738. doi:10.1038/nature09406.

603 [21] L. Sun, X. Zeng, C. Yan, X. Sun, X. Gong, Y. Rao, et al., Crystal structure of
604 a bacterial homologue of glucose transporters GLUT1–4, Nature. 490 (2012)
605 361–366. doi:10.1038/nature11524.
606
607 [22] Y. Huang, M.J. Lemieux, J. Song, M. Auer, D.-N. Wang, Structure and
608 mechanism of the glycerol-3-phosphate transporter from *Escherichia coli*,
609 Science. 301 (2003) 616–620. doi:10.1126/science.1087619.
610
611 [23] J. Abramson, I. Smirnova, V. Kasho, G. Verner, H.R. Kaback, S. Iwata,
612 Structure and mechanism of the lactose permease of *Escherichia coli*, Science.
613 301 (2003) 610–615. doi:10.1126/science.1088196.
614
615 [24] B.W. Matthews, Solvent content of protein crystals, J. Mol. Biol. 33 (1968)
616 491–497. doi:10.1016/0022-2836(68)90205-2.
617
618 [25] I. Moraes, G. Evans, J. Sanchez-Weatherby, S. Newstead, P.D.S. Stewart,
619 Membrane protein structure determination — the next generation, Biochim.
620 Biophys. Acta. 1838 (2014) 78–87.
621